Jurnal Teknologi, 52 Mei 2010: 103–115

RESOLUTION AND NOISE PROPERTIES OF CMOS AND CR DIGITAL RADIOGRAPHY SYSTEMS

KHAIRUL ANUAR MOHD SALLEH[1], WAN MUHAMAD SARIDAN WAN HASSAN[2], AB. RAZAK HAMZAH[3]

Abstrak. Seiring dengan perkembangan teknologi perkomputeran dan pemprosesan imej, radiografi industri berbentuk konvensional telah bertukar arah kepada radiografi industri berasaskan digital. Dalam kajian ini, dua jenis alat radiografi industri digital untuk ujian tanpa memusnah (NDT), iaitu *complimentary metal oxide semiconductor* (CMOS) dengan jarak piksel 50 μm dan *computed radiography* (CR) dengan jarak piksel 25 μm telah diuji dan diukur untuk menentukan kesesuaiannya dalam NDT. Pengukuran fungsi hantaran modulasi (MTF) dan spektrum kuasa hingar (NPS) telah dilakukankan ke atas kedua-dua peralatan ini bagi menilai kualiti imej yang dihasilkan. Daripada pengukuran dan pengiraan yang dilakukan, purata MTF untuk CR dan CMOS pada modulasi 20% ialah 4.48 kitar/mm dan 2.83 kitar/mm. Untuk NPS pula keputusan menunjukkan CMOS memberikan hingar yang lebih tinggi daripada CR tetapi CR mempunyai keupayaan MTF yang lebih pada ukuran 20% modulasi. Daripada pengukuran dan pengiraan yang dijalankan, dapatlah dikatakan bahawa untuk menjalankan satu ujian NDT, pengguna perlu tahu keupayaan sebenar sesebuah alat dan bagaimana ia dibina supaya ujian NDT memberi gambaran tepat ke atas sesuatu sampel atau barangan yang diuji.

Kata kunci: Ujian tanpa memusnah (NDT); radiografi industri berasaskan digital (IDR); fungsi hantaran modulasi (MTF); spektrum kuasa hingar (NPS)

Abstract. Due to development of computer technology and image processing, conventional industrial radiography has changed to digital radiography system. In this study, two types of industrial digital radiography (IDR) modules for non destructive testing (NDT), namely complimentary metal oxide semiconductor (CMOS) with 50 μm pixel pitch and computed radiography (CR) with 25 μm pixel pitch have been evaluated for NDT applications. The modulation transfer function (MTF) and noise power spectrum (NPS) measurement and calculation were adapted in order to evaluate the image quality of IDR images. From the measurement and calculation, the averaged MTF for CR and CMOS at 20% modulation are 4.48 cycles/mm and 2.83 cycles/mm, respectively. NPS measurement and calculation show that CMOS produced higher noise than CR. The CR system has lower and more stable NPS but has lower modulating capability at 20% compared to the CMOS system. The

---

[1&3] Non-Destructive Testing Group, Industrial Technology Division, Malaysian Nuclear Agency, 43000 Bangi, Kajang, Selangor Darul Ehsan.
Tel: 60389250510. Fax: 60389250907. Email: khairul_anuar@nuclearmalaysia.gov.my & razak_hamzah@nuclearmalaysia.gov.my

[2] Department of Physics, Faculty of Science, Universiti Teknologi Malaysia, 81310 Skudai, Johor Darul Ta'zim.
Tel: 6075534191. Fax: 6075566162. Email: wmsaridan@utm.my

study shows that in order to perform NDT by using the evaluated modules, the user must know the true capability of the system and how it is designed for specific application and discontinuity detection.

Keywords: Non destructive testing (NDT); industrial digital radiography (IDR); modulation transfer function (MTF); noise power spectrum (NPS); complimentary metal oxide semiconductor (CMOS) and computed radiography (CR)

1.0 INTRODUCTION

Image quality is one of the important aspects in industrial radiography. The concept of image quality has undergone a transformation with the widespread use of industrial digital radiography (IDR) systems. The new imaging modalities, such as computed radiography (CR) and complimentary metal oxide semiconductor (CMOS) flat panel are beginning to replace standard screen-film imaging systems. There are two main quantitative parameters that are traditionally used as part of evaluation for radiographic image quality, namely the modulation transfer function (MTF) and noise power spectrum (NPS). The two quantities can be combined to produce the detective quantum efficiency (DQE), which is the currently accepted measure for imaging system performance [1].

In this work, two digital radiography systems namely CMOS and CR are studied and evaluated in terms of spatial resolution and noise property by performing the two measurement and calculation.

2.0 PRINCIPLE OF MEASUREMENT

The MTF represent the maximum ability of IDR modules for transferring subject contrast, to the final image as a function of spatial frequency. The MTF measurement use an edge spread function method as it provides convenient measurement and portray better accuracy at low frequencies compared to other techniques [1]. The MTF is commonly measured for an evaluation of the spatial resolution properties of screen-film systems [2]. The MTF as defined by Rossmann [3] is a measure of image deterioration due to optical factors, such as diffusion of image forming radiation. It is a measurement of sharpness for imaging system for component of a system and measured in cycles/mm or lp/mm. MTF also describes the transfer of sinusoidal inputs in spatial frequency domain. Mathematically, the MTF is defined as the Fourier transform of a line spread function (LSF), $l(x)$. A response of an imaging system towards a single line input creates the LSF which is the differentiation of the edge spread function, $e(x)$;

$$l(x) = \frac{d}{dx} e(x) \tag{1}$$

In this work, the edge spread function, *e*(*x*) is generated by using a sharp edge image produced from radiographed phantoms. The equation pertaining to *M*(*u*) is as follows [4]:

$$M(u) = \left| \int_{-\infty}^{\infty} l(x) e^{-2\pi i u x} \, dx \right| \tag{2}$$

The NPS provides the mean of characterizing image noise and plays a central role in the ultimate measure of image quality; the number of noise-equivalent quanta, (NEQ) and Fourier analysis is the gold method in determining the NPS [5]. Noise in images is recognized as an important factor in determining image quality. The optical density fluctuations of digital data are collected and calculated to produce the NPS curve. The following equation is applied [5]:

$$NPS(u,v) = \lim_{\substack{x \to \infty \\ y \to \infty}} \frac{1}{4xy} \overline{\left| F_D(u,v) \right|^2} \tag{3}$$

where

$$F_D(u,v) = \int_{-x}^{x} \int_{-y}^{y} \Delta D(x,y) \exp\left\{-2\pi i (ux + vy)\right\} dx dy \tag{4}$$

The NPS data is plotted against spatial frequency which in according to [6]:

$$\text{Spatial frequency} = \sqrt{u^2 + v^2} \tag{5}$$

where *u* and *v* are spatial frequencies in the Fourier domain corresponding to *x* and *y* in the spatial domain. The MTF and NPS are limited to frequencies below the Nyquist frequency which is related to the size of the pixels in the image as:

$$\text{Nyquist frequency} = \frac{1}{2 \times \text{pixel pitch}} \tag{6}$$

3.0 MATERIALS AND METHODS

The IDR modules which were studied are as tabulated in Table 1. The selected modules are used as IDR inspection tools and widely available in the market. The complimentary metal oxide semiconductor flat panel detector (CMOS C7942CA, Hamamatsu, Japan) and computed radiography (HDCR, Dürr NDT, Germany) images were obtained by using typical industrial radiography setup for joined plate inspection, single wall single image technique and test phantoms.

Table 1 Basic physical character of IDR module

IDR Module	**CMOS flat panel detector**		**Computed radiography**	
Pixel Size (μm)	50		25	
Field size (pixels)	2240 × 2368		9487 × 3930	
Data acquisition	kV	mA	kV	mA
Analogue Digital Converter (bit)	12	3	120	3
	12		12	

The exposure parameters which were used on CMOS flat panel and CR system was 120 kV tube potential, 3 mA current and 1 minute 7 seconds exposure time for CMOS and 9 seconds for CR to ensure the same quality achieved as D7 type film for 10 mm weld crown cap and plate height. The 120 kV was chosen because it is the kV chosen for some of the most popular asymmetric screen film work and the most suitable parameter suggested by the exposure chart. The X-radiation exposures were made in industrial X-radiation exposure room with 300 kV Seifert constant potential panoramic X-ray tube (Eresco MF3, General Electric Inspection Technology (GEIT), Germany) and the generator is Seifert Eresco Portable X-ray Unit Digital Control from GEIT. A special diaphragm from Seifert was used for this purpose to ensure the path of the X-rays goes directly to the object under test. A source to object (SOD) distance was chosen as 700 mm to reduce errors caused by geometrical unsharpness and misalignment of the X-ray beam with the test phantom. A two cm thick lead sheet was used to reduce back scatter radiation. The acquisition of images was done by using software which was provided by the manufacturer of the system (Dürr D-Tect, Dürr NDT, Germany) and the acquired images were saved into computer with a unique file name (.XYZ file format). Two test phantoms were used in the experiment i.e.:

(i) A specially custom made platinum plate with 99.95% purity, thickness of 0.5 mm, 75 mm width and 100 mm length;

(ii) Double wire image quality indicator (IQI) for determination of image unsharpness (EN 462-5 Duplex IQI, IE-NDT Ltd, London).

The test phantoms were located at the top of the detector under test. The platinum plate has sharp edge purposely polished to obtain the best possible MTF. The image retrieval was performed by using ImageJ (National Institutes of Health, New York, USA). The software gives the user freedom to define, save and retrieve defined region of interest at same location whenever the same image being called i.e. the image of modules under test. Further work was carried out by using Igor Pro 5.02 (WaveMetrics, Ohio, USA). It was used for analyzing MTF and NPS measurement and calculation. In performing the MTF measurement, four flat field of the sharpest platinum plate edge were defined. The sharp edge image which was the region of interest (ROI) of size 181 (v) × 265 (h) data was manually drawn from the image of each module.The four ROI was selected randomly from each image in order to portray the randomness in unsharpness and defect on object under test. The size and coordinate of the ROI was saved and retrievable by using ROI manager from analyze function. The process was divided in two parts, the manual handling using ImageJ and the automatic handling using Igor Pro 5.02. For manual handling, the selected ROI were duplicated and saved into two forms which were the image itself (CR_ROI#1.tiff, CR_ROI#2.tiff, CR_ROI#3.tiff, CR_ROI #4.tiff) and as text format (CR_ROI#1.txt, CR_ROI#2.txt, CR_ROI#3.txt and CR_ROI#4.txt). A computer procedure for automatic handling was written purposely to calculate and fit the MTF curve. The computer procedure is executable in Igor Pro 5.02 and the flow is shown in Figure 1. Each .txt file was recalled as waves in Igor Pro 5.02. By doing this, specific file name shall be used for each module and new folders for distinctive directories shall be created for each. The number of waves depends on numbers of data set available in the .txt file; in this case, four 181 (v) × 265 (h) waves were created for each directory. The automatic handling was used to average the waves to produce ESF, $e(x)$ which was a single wave. The command for CR_ROI#1 is as follow:

'Average_CR_ROI#1'=('SUM_CR_ROI#1_0-50'+'SUM_CR_ROI#1_51-101'+'SUM_CR_ROI#1_102-147'+'SUM_CR_ROI#1_148-181')/182

Equation 1 was used to obtain the LSF, $l(x)$ using the command:

Differentiate 'Average_CR_ROI#1'/D='Average_CR_ROI#1_DIF

The LSF was Fourier transformed by using Equation 4. The output was normalised and plotted against spatial frequency. Since the spatial frequency depends on pixel pitch, a 25 micron and 50 micron pixel pitch will give different spatial frequency interval for the MTF curve. For fast Fourier transformation of 256 data, the spatial frequency interval of 25 micron pixel pitch is $\Delta u = \frac{1}{256 \times 0.025}$ = 0.15625 mm^{-1}. Thus the tick marks on the u axis are 0, Δu, $2\Delta u$, $3\Delta u$, ... equivalent to 0, 0.1562, 0.312, 0.467… mm^{-1}. For 50 micron pixel pitch, the frequency interval is $\Delta u = \frac{1}{256 \times 0.05}$ = 0.078125 mm^{-1}. Thus, the tick marks on the u axis are 0, Δu, $2\Delta u$, $3\Delta u$,… equivalent to 0, 0.07 8, 0.156, 0.234… mm^{-1}.

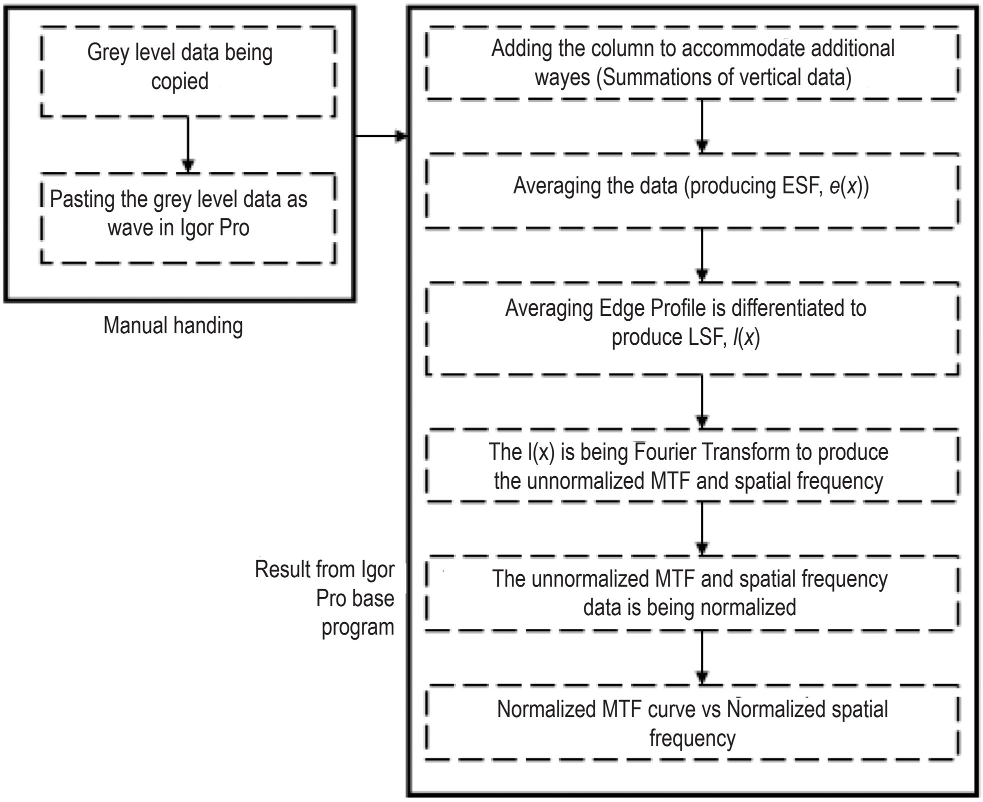

Figure 1 Flow of the MTF measurement and calculation

In order to determine the NPS, 10 flat-field free beam images of each module with 256 (v) × 256 (h) pixels were acquired as region of interest (ROI) by using ImageJ. The

ROI was saved into two forms which were the image itself (.tiff) and as text format (.txt). The sizes and coordinates of the ROI were duplicated and saved.

The ROI was retrievable by using ROI manager from analyze function of ImageJ. Another process function which exists in ImageJ was used to Fourier transform the image data in accordance with equations 3 and 4 which estimates the noise power spectrum of the recorded image noise. The data were then saved into two forms namely the .tiff format and .txt text format. The averaging procedure was performed by using Microsoft Excel and the averaged product was saved in text format. The text format was retrieved by using ImageJ and this gave the 2D NPS data. A profile for u_{128} to u_{256} gave the NPS curve. Thus 2D NPS was obtained by the 2D Fourier transformation of noise data. The noise power along u axis was taken as the NPS curve. The data was then saved as .txt format and plotted against its spatial frequency. Figure 2 shows the diagram in performing the NPS measurement.

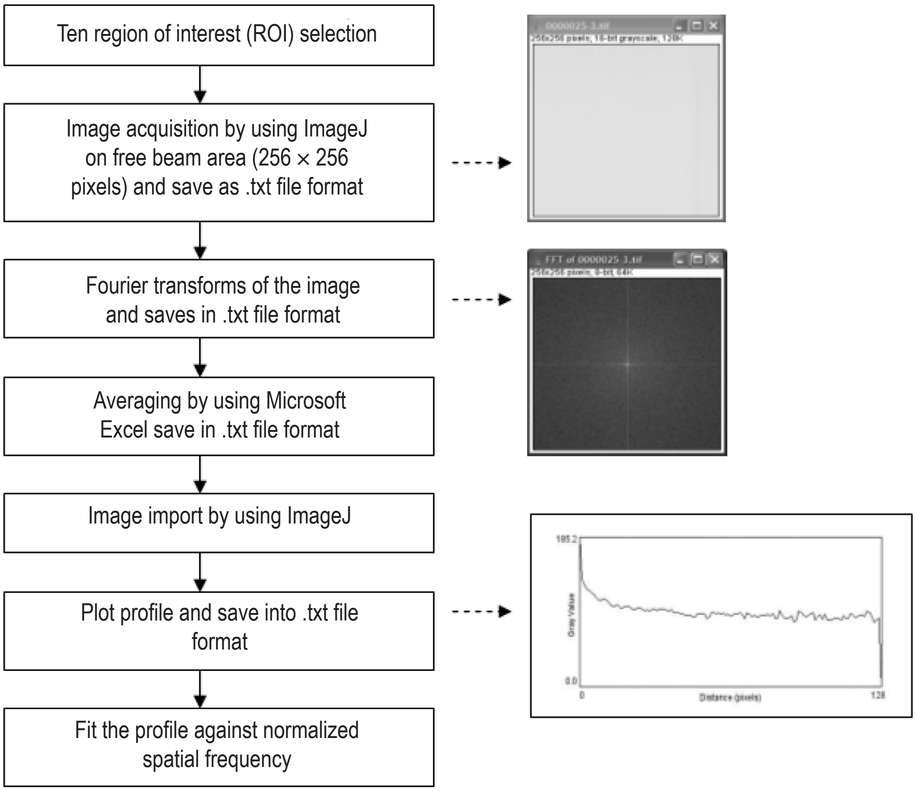

Figure 2 The flow procedure in performing the NPS measurment by using 2 dimensional (2D) Fourier transform method

4.0 RESULT AND DISCUSSION

4.1 Modulation Transfer Function (MTF)

Figures 3(a), (b) and (c) show the results of measurements and calculations done on Computed Radiography (CR) 25 μm system. According to equation 6, the limiting frequency (Nyquist frequency) is 20 cycles/mm. The measurements and calculations performed on the CR correspond well with the results of Samei [1], Flynn *et al.* [12] and Dobbins *et al.* [6] who studied older generation of CR system.

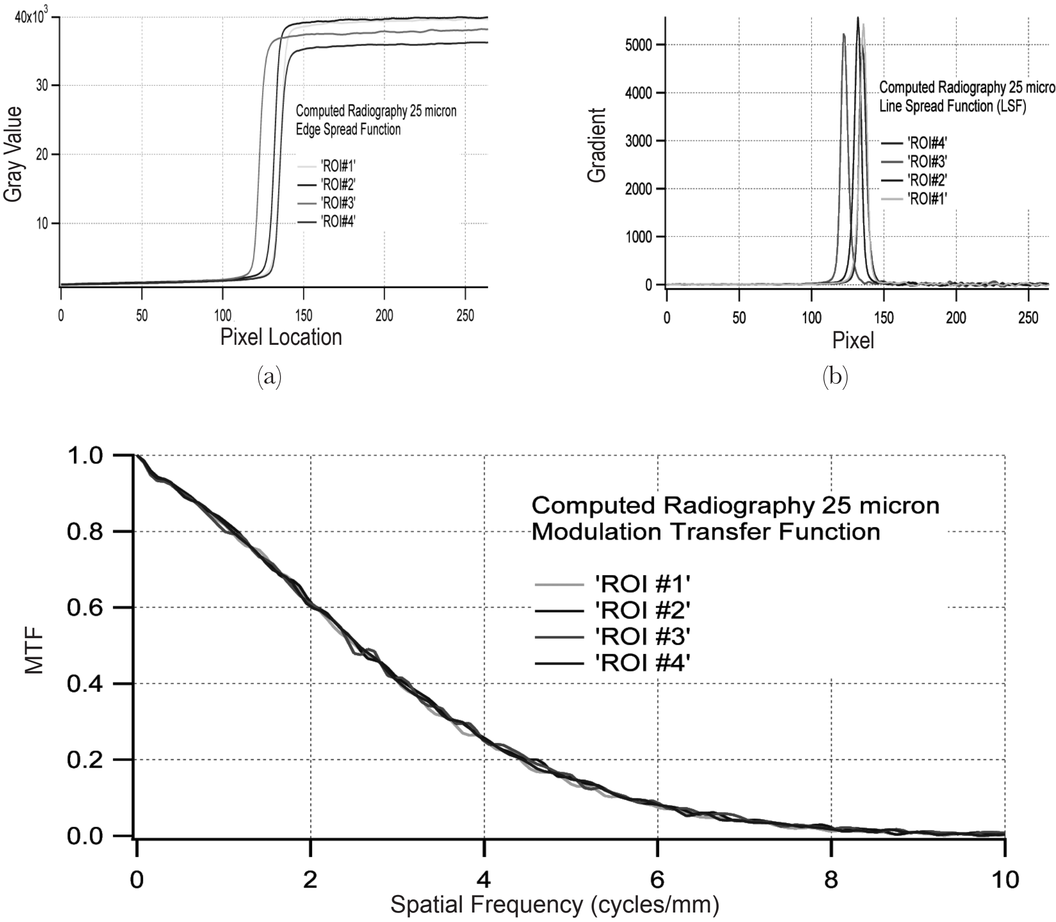

(a) (b)

(c)

Figure 3 (a) Edge spread function, (b) Line spread function and (c) Modulation transfer function of four regions of interest in Computed Radiography 25 μm system

Figures 4(a), (b) and (c) show the results of measurement and calculation done on CMOS 50 μm flat panel system. According to equation 6, the limiting frequency (Nyquist frequency) is 10 cycles/mm. The patterns of MTF curves for the CMOS flat panel correspond well with the results of Kim *et al.* [8], Stolin *et al.* [9] and Kim *et al.* [10].

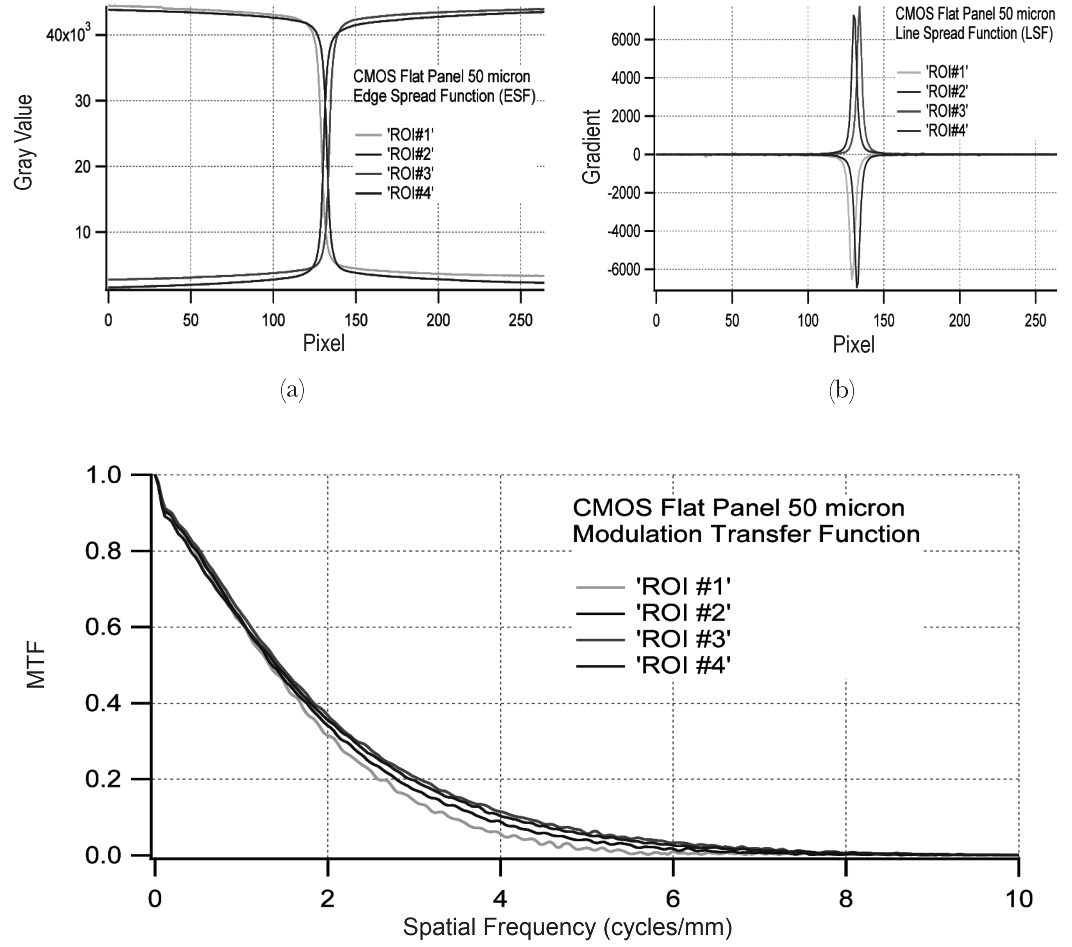

(a) (b)

(c)

Figure 4 (a) Edge spread function, (b) Line spread function and (c) Modulation transfer function of four regions of interest of CMOS flat panel 50 μm system

Figures 3–4 (a), (b) and (c) show the results of measurements and calculations done on 25 μm CR and 50 μm CMOS system.

In agreement with work of Dobbins *et al.* [6], the MTF curves as illustrated in Figure 3 (a) of the CR 25 μm correspond similarly to the CR 200 μm system which was tested and the 20% modulation is about 2 cycles/mm. The CR 25 μm system however, modulates approximately 4.5 cycles/mm at 20%. Zscherpel [7], who performed the same measurement on the CR 25 μm, obtained $\mathrm{MTF}_{20\%}$ at 7 cycles/mm. Fujita *et al.* [4] in their work mentioned that one of the degrading factors in CR MTF measurement is glaring factor, from scattering of light during imaging plate laser scanning. The glare effect might reduce the contrast of the image leading to lower modulation. The difference in terms of contrast between the two images is however, agreed by Zscherpel [7]. Another factor which contributes to the difference is due to the number of sampled data where the 7 cycles/mm of Zscherpel [7] is a result of 59 × 1237 pixels ROI (256 × 256 pixels). The four ROI were not giving significant difference even though they were from different part of the image. This indicates any part of the CR detector has the same spatial resolution property in imaging terms. Figure 3(a) and (b) show differences when the ESF and LSF were sampled differently and yet found no problem in having almost the same MTF curves. Figure 3(a) illustrates the difference in contrast for each ROI. The ESF for ROI #3 in Figure 3(a) (red colour) shows a lower contrast image and the same for the ESF of ROI #4 (blue colour). This was due to non-completed or not properly "flashed" imaging plate which had a ghost image from previous high exposure. However the MTF curves produced did not show noticeable discrepancy. The ESF curves in Figure 3(a) show very smooth increasing grey value and do not contain aliasing effect.

Figure 4(c) shows a comparison of MTF for four ROI which are plotted on the same graph. ROI #1 has the lowest MTF at spatial frequency of 1.8–6 cycles/mm. The MTF curves of the CMOS flat panel system suggest that the system will not be able to give the same spatial resolution in some area as there is also small difference portrayed on ROI #2. The fast dropping MTF curve is majorly due to unsharpness of the scintillator screen used in the radiation to visible light converter. It can be seen that in Figure 4(a) and (b), different sampling technique, i.e. different direction in plotting the ESF might be the reason to why the ROI #1 and ROI # 2 as fast dropping MTF curves. It gives an idea on which position to place the object of interest or test sample. The image correcting factor is important before the MTF measurement is performed because the CMOS flat panel is sensitive to differences in exposure parameters. Stolin *et al.* [9] measured the older version of the flat panel with 48 μm pixel pitch by using a slit method and obtained approximately 3–4 cycles/mm at 20% modulation and this is comparable with MTF of ROI #3. The slit method used by Stolin *et al.* [33] sampled only one line of pixels to obtain the LSF where else; our ESF were average of 256 pixels. In contrast to result obtained by Kim *et al.* [8] and Kim *et al.* [10], the measured MTF at 20% modulation is approximately 4–5 cycles/mm which is higher. The X-ray source which was used in the experiment are Microfocus X-ray source with 50 μm focal spot size [8]. One of the reasons that contribute to unsharpness is the geometrical unsharpness (μ_g) and focal spot size in one of the factor which contributes to the μ_g and lower MTF as in Figure 4(b). The X-ray source which was used in this work is a panoramic type 360 kV Seifert constant potential with wide angle focal spot, thus introducing a high μ_g and limiting the MTF.

Table 2 shows the estimation of spatial frequency at which 20% modulation, $\text{MTF}_{20\%}$ occurred. The average $\text{MTF}_{20\%}$ for each modality is also given in the table The CMOS flat panel detector gave the lowest $\text{MTF}_{20\%}$ because of unsharpness of the scintillating material, thus limiting the modality to only certain application of industrial radiography. The CR 25 μm system has a better spatial resolution than the CMOS. Overall, the MTF estimates were comparable to previously obtained results by Dobbins *et al.* [6].

Table 2 Estimation of 20% modulation from each modality on each four regions of interest

No.	**Modalities**	**$\text{MTF}_{20\%}$ (cycles/mm)**				
		#1	**#2**	**#3**	**#4**	**Average**
1	Computed Radiography (CR) 25 μm	4.44	4.53	4.50	4.45	4.48
2	Complementary Metal-Oxide Semiconductor (CMOS) Flat Panel 50 μm	2.58	2.80	3.04	2.93	2.83

Figure 5 shows the averaged MTF curves for each module. The fastest dropping curve at the lowest spatial frequency goes to the CMOS flat panel with 50 μm pixel pitch.

4.2 Noise Power Spectrum (NPS)

Figure 6 shows the relative NPS of the two modalities for the main spatial frequency axes. The result shows that the CR flat panel has noise power that is distributed about equally to all frequencies. Figure 6 also shows that CR has lower noise power spectrum than the CMOS type detector for low spatial frequency. It can be seen from Figure 6 that in order to have a better image or to see visually hard to sees discontinuities with

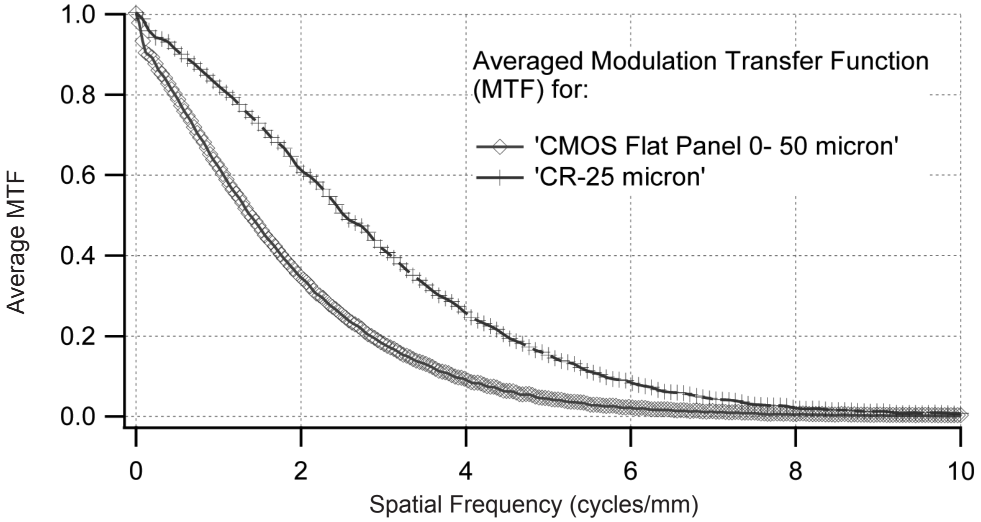

Figure 5 Averaged modulation transfer function of CMOS flat panel and CR systems

a low noise along most of the spatial frequency, the CR would be the better choice. In agreement with works done by Maryellen *et al.* [11] and Dobbins *et al.* [6], the NPS curve obtained in this work agreed well with results obtained from the published document.

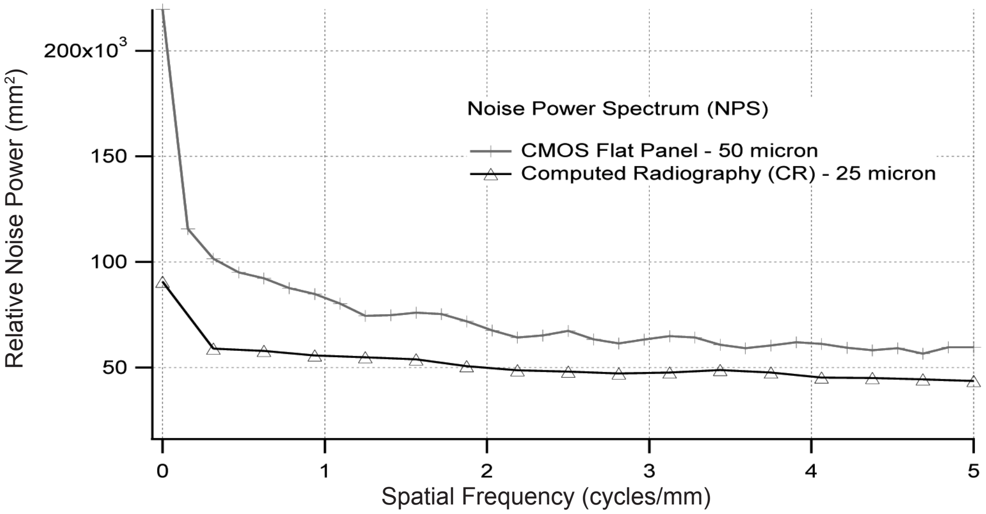

Figure 6 The noise power spectrum curves of the CMOS flat panel and CR systems up to 5 cycles/mm

5.0 CONCLUSION

We have measured the resolution and noise properties of CMOS flat panel and CR industrial digital radiography systems. In obtaining a high quality IDR images for application such as searching for discontinues in weld joint in NDT, one must know the true capability of the system and how the system is designed. It is not enough to have only one parameter such as the MTF as the quality parameter, but other parameter such as the level of noise also plays important role in having high quality image. The NDT practitioner must know in which conditions, certain modalities is used especially when it involves a very critical inspection and needs a precise indication of discontinuities.

ACKNOWLEDGEMENT

Authors would like to thank Dr. Uwe Zscherpel and Dr. Oleksandr Alekseychuk of Federal Institute for Materials Research and Testing (BAM), Berlin for assistance in acquiring the digital images and Research Management Centre (RMC) of Malaysian Nuclear Agency for funding this work.

REFERENCES

[1] Samei, E. 1997. The Performance of Digital X-ray Imaging Systems in Detection of Subtle Lung Nodules. PhD Thesis.

[2] ICRU – Modulation Transfer Function of Screen-Film System, ICRU Report 41, 1986. *International Commission on Radiation Units and Measurements, Bethesda*. Maryland, USA.

[3] Rossmann, K. 1964. Measurement of the Modulation Transfer Function of Radiographic Systems Containing Fluorescent Screens. *Phys. Med. Biol*. Vol. 9(4): 551–557.

[4] Dainty, J. C. and Shaw, R. 1974. *Image Science*. London, Academic Press.

[5] Dobbins III, J. T. and Boone J. M. 1998. A Simplified Method of Estimating Noise Power Spectra. *Physics of Medical Imaging.* Proc. SPIE 3336. 243–250.

[6] Dobbins III, J. T., Ergun, D. L., Rutz, L., Hinshaw, D. A., Blume, H. and Clark, D. C. 1995. DQE(f) of Four Generations of Computed Radiography Acquisition Devices. *Medical Physics*. 22: 1581–1593.

[7] Uwe Zscherpel, 2002. Private conversation.

[8] Kim, K. H., Chae, J. S., Yuk, S. W., Kim, Y. S., Chi, Y. K. and Cho. G. 2003. Evaluation of CMOS APS Imager for Digital Radiography and Mammography. *IEEE*. Vol.5: 3190–3194.

[9] A.V. Stolin, B.K. Kundu, D.J. Pole, and M.B. Williams. 2004. Characterization and Comparison of X-ray Detectors for Use in Small Animal Imaging. *IEEE*. Vol. 6: 3480–3483.

[10] K. H. Kim, and G. Cho. 2003. The Effect of Direct X-ray on CMOS APS images for Industrial Application. *IEEE*. Vol.2: 1425–1429.

[11] Maryellen G. L., Doi K. and Metz C. E. 1984. Investigation of Basic Imaging Properties in Digital Radiography. 2. Noise Wiener Spectrum. *Med. Phys*. 11(6): 797–805.

[12] Flynn, M. J. and Samei, E. 1999. Experimental Comparison of Noise and Resolution for 2k and 4k Storage Phosphor Radiography Systems. *Med Phys*. 26: 1612–1623.